

LLM Judges Have Dark Current: A Psychometric Datasheet for LLM-as-a-Judge Evaluation

Hiroyasu Usami¹, Keisuke Hara¹, Ayato Tsuboi¹, and Naohiko Matsuda²

¹ Department of Computer Science, Graduate School of Engineering, Chubu University, Kasugai, Aichi 487-8501, Japan

² Mitsubishi Heavy Industries, Ltd., Research & Innovation Center, Heat Transfer Research Department, Takasago, Hyogo 676-8686, Japan
 usami@fsc.chubu.ac.jp
<https://usamilab.org>

June 12, 2026

Abstract

LLM-as-a-judge systems are now routinely used for open-ended model evaluation, where human preference annotation is costly, slow, and difficult to reproduce. Yet these judges are often reported as scalar accuracy, win-rate, or agreement devices. We argue that a judge should instead be reported as a measurement instrument. We introduce a Judge Datasheet protocol that measures dark current under true-vacuum inputs, stable cross-sensitivity to same-quality surface variation, positional false preference, target sensitivity on a controlled quality ladder, and the criterion or operating point induced by tie instructions. The direction-stability decomposition reveals that apparent $\Delta 0$ preference can be stable surface response or disguised position bias. In a three-judge open-weight case study, Llama-3.1-8B shows high dark current and presentation-conflicted $\Delta 0$ behavior, Qwen2.5-14B is vacuum-clean and target-sensitive but mixes stable and positional over-discrimination, and Qwen2.5-32B is vacuum-clean with low stable cross-sensitivity and low positional false preference. A strict tie criterion eliminates Qwen32B $\Delta 0$ false preference but absorbs marginal $\Delta 1$ target signals into ties while preserving $\Delta 5$ sensitivity. The results show that prompting moves the criterion, not the resolution. We do not claim that the downstream mechanism hypothesis that motivated this work is confirmed; the contribution is a metrological protocol for measuring the measuring device before downstream claims are made.

1 Introduction

LLM-as-a-judge evaluation has become a practical default for comparing open-ended model outputs. In current LLM development practice, open-ended model comparison often relies on automatic judges because human evaluation is expensive, slow, and hard to reproduce at benchmark scale. This makes the judge part of the evaluation infrastructure, not merely a convenient scorer. The attraction is clear: a judge can read natural language, apply task-specific criteria, and produce a preference without first reducing the answer to a narrow automatic metric. But once a judge is used to validate another system, the judge itself becomes a measurement instrument. It can have background response in the absence of signal, sensitivity to the intended construct, cross-sensitivity to nuisance variation, position bias, and an operating criterion that determines when a weak signal is reported as a preference or as no preference.

This work originated from a downstream study of orientation in LLM evaluation. That downstream mechanism is not tested here; the present paper measures whether the judge is calibrated enough to support such claims. We use ChiralityEval as the motivating project name for that downstream line, but the contribution here is judge metrology rather than mechanism validation.

We define *dark current* as false preference under true-vacuum inputs, including empty answers, whitespace, and identical non-empty answers. We define *positional false preference* as an apparent preference driven by the presentation slot rather than candidate content. We define *stable cross-sensitivity* as stable response to non-target but real surface-form variation under same-quality $\Delta 0$ comparisons after presentation order has been canonicalized. We define *target sensitivity* as detection of intended quality differences on a constructively controlled ΔQ ladder. Finally, we define *criterion* as the tie/preference operating point induced by the instruction and prompt.

Our contributions are fivefold:

- **Judge Datasheet protocol.** We introduce a Judge Datasheet protocol for LLM-as-a-judge systems, combining A0 true-vacuum tests, A1 controlled quality ladders, and criterion-shift probing.
- **Direction-stability decomposition.** We make $\Delta 0$ direction-stability decomposition a first-class measurement: raw same-quality false preference is separated into stable cross-sensitivity, positional false preference, one-sided commit, other conflict, and no-preference at the canonical-pair level.
- **Controlled stimulus ladder.** We construct a prefix-chain checklist stimulus ladder with Pareto dominance, $\Delta 0$ same-subset and different-subset controls, filler controls, and validity gates.
- **Three-judge case study.** We present a case study of Llama-3.1-8B, Qwen2.5-14B, and Qwen2.5-32B, showing that they occupy different metrological profiles.
- **Criterion-shift probe.** We show that strict tie prompting moves the criterion: it eliminates Qwen32B $\Delta 0$ false preference but absorbs marginal $\Delta 1$ target signals into ties while preserving $\Delta 5$ sensitivity.

The central claim is deliberately narrow. We do not claim that the downstream mechanism hypothesis or an orientation mechanism is confirmed. We do not claim a broad size-family trend, a universal judge, or a human-ground-truth result. We claim that LLM judges require multi-axis measurement before they are used as evidence-bearing instruments.

2 Related Work

LLM-as-a-judge reliability and IRT. Prior work has diagnosed LLM judges through observational latent-trait modeling and benchmark-level reliability. Choi et al. use item-response theory to diagnose LLM-as-a-judge reliability from observational response patterns [1]. We complement this line with an experimental psychophysics protocol: constructively controlled stimulus strength, true-vacuum inputs, direction-stability tests, and direct criterion manipulation.

Evaluation infrastructure and automatic judges. Large-scale evaluation frameworks such as HELM and BIG-Bench frame evaluation as infrastructure for measuring language-model capabilities across tasks and risks [2, 3]. In parallel, LLM-based automatic evaluators such as MT-Bench/Chatbot Arena and Length-Controlled AlpacaEval made open-ended evaluation cheaper and

Table 1: Judge Datasheet protocol components.

Component	Purpose	Reported quantities
A0 true vacuum	Measures false preference when no evaluative signal is present, including empty, whitespace, and identical answers.	Dark current, non-preference, schema validity.
A1 quality ladder	Measures target sensitivity on a constructively controlled prefix-chain checklist ladder.	$P(\text{correct} \mid \Delta Q)$, Δ_{75}^* , SDT quantities.
$\Delta 0$ controls	Separates same-quality surface variants from different-subset equal-cardinality variants.	Raw false preference, stable cross-sensitivity, positional false preference, no-preference.
Criterion probe	Moves the tie/preference operating point without changing the underlying stimulus ladder.	Tie absorption, low- Δ miss rate, high- Δ preservation.
Validity gates	Prevents syntactic success from being treated as scientific validity.	Parse success, schema validity, semantic validity, hidden-metadata checks.

faster, while also exposing judge-specific biases such as position, verbosity, and length sensitivity [4, 5]. Practical evaluation frameworks such as OpenAI Evals further normalize evaluation loops as part of model development [6]. Our work focuses on the measuring side of this infrastructure: before a judge score is used as evidence, the judge itself should have a datasheet.

Signal detection and criterion. Signal detection theory separates sensitivity from criterion. Cacioli frames LLM decisions in SDT terms and develops a temperature-criterion analogy [7]. We use SDT framing operationally for pairwise judge decisions and prompt-induced criterion shifts: a prompt can shift the tie/preference operating point without increasing the resolution of the underlying measurement.

Biases in judge preferences. LLM judges are known to exhibit position, verbosity, self-preference, and order effects. MT-Bench and Chatbot Arena popularized LLM-as-a-judge evaluation while documenting position, verbosity, and self-enhancement biases [4]. Shi et al. systematically study position bias and its dependence on comparison conditions [8]. Yang et al. study self-preference bias with equal-quality comparisons and mitigation strategies [9]. Prior position-bias work often measures aggregate order effects or marginal slot preferences. We complement it with an operational $\Delta 0$ direction-stability test that separates content-stable preference from slot-stable preference at the canonical-pair level.

Documentation and datasheets. Datasheets for Datasets and Model Cards established structured disclosure practices for datasets and models [10, 11]. Our unit of documentation is the evaluator itself. A Judge Datasheet separates dark current, position-driven false preference, stable cross-sensitivity, target sensitivity, and criterion so that downstream claims do not silently inherit unmeasured judge behavior.

3 Judge Datasheet Protocol

3.1 Notation

Let $z = \{u, v\}$ be a canonical unordered content pair. A presentation order is $o \in \{(u, v), (v, u)\}$, where the two contents are assigned to slots 1 and 2. The judge returns a slot-level output $J(o) \in \{1, 2, \text{tie}\}$. We map the slot-level output back to canonical content identity as $W_J(o) \in \{u, v, \text{tie}\}$. The order-reversal operator is $\pi(u, v) = (v, u)$. Slot identity and content identity are not the same: direction-stability metrics are computed only after mapping slot outputs back to canonical candidate identity. All direction-stability metrics are computed after mapping slot winners back to canonical content identities; slot-level equality and content-level equality mean opposite things under order reversal.

3.2 Metrics at a glance

Table 2: Metrics at a glance. This compact main-text view gives the metric level and direction of concern; protocol and denominator details appear in Appendix Table 7. Bad direction is relative to the controlled checklist construct rather than a moral judgment. Some axes are construct-relative: stable cross-sensitivity may be useful if style or surface form is part of the target construct.

Term	Symbol	Level	Measures	Bad direction
Dark current	DC	call	false preference with no evaluative signal	higher
Raw Δ_0 false preference	RFP ₀	call	any non-tie on same-quality same-subset pairs; raw, not cross-sensitivity	higher
Stable cross-sensitivity	SCS	canonical pair	content-stable direction under surface variation	construct-dependent
Positional false preference	PFPP	canonical pair	same presentation-slot choice under order reversal	higher
No-preference	NP	call or pair	tie or valid abstention	construct-dependent
Target sensitivity	$P_{\text{correct}}(\Delta Q)$	call	correct selection of the Pareto-dominant prefix-chain candidate	lower
Detection threshold	Δ_{75}^*	ladder fit	smallest ΔQ where isotonic target sensitivity reaches 0.75	higher
Criterion / operating point	C_J / tie rate	condition	prompt-induced tie/preference boundary	no universal direction
Miss-by-tie	MBT	call	target signal not selected because the judge returns tie	higher when signal should be detected

How to read the metrics. Raw Δ_0 FP is not cross-sensitivity. Stable cross-sensitivity requires content-stable direction under order reversal. Positional false preference requires slot-stable choice under order reversal. RFP₀ averages two presentation-order calls per canonical pair; SCS, PFP, OSC, and Other are canonical-pair decomposition terms combined by Eq. 7. A high tie rate is not always bad; in true vacuum it is desirable. $\Delta_{75}^* \leq 1$ is not exactly 1; it is left-censored by the ladder granularity. The strict criterion arm is not a new judge and does not have dark-current measurement unless A0 is rerun under that prompt. Reference/API judges are external comparators, not ground truth.

3.3 Metric definitions

Let \mathcal{V} be the true-vacuum set and let J_{tie} denote the tie-allowed judge protocol. True-vacuum inputs include empty, whitespace, and identical non-empty pairs. Dark current is the non-abstaining false-

preference rate under the tie-allowed protocol:

$$\text{DC}(J) = \mathbb{E}_{(u,v) \in \mathcal{V}} [\mathbf{1}\{W_J(u, v) \neq \text{tie} \wedge W_J(u, v) \neq \text{abstain}\}]. \quad (1)$$

In this paper, valid abstention is treated as no-preference for this axis.

Let \mathcal{D}_0 be the $\Delta 0$ same-subset canonical-pair set. Raw $\Delta 0$ false preference is a call-level non-tie rate, written as the average of the two presentation-order calls for each canonical pair:

$$\text{RFP}_0(J) = \mathbb{E}_{(u,v) \in \mathcal{D}_0} \left[\frac{1}{2} (\mathbf{1}\{W_J(u, v) \neq \text{tie}\} + \mathbf{1}\{W_J(v, u) \neq \text{tie}\}) \right]. \quad (2)$$

This quantity includes stable, positional, one-sided, and conflict components. We therefore do not call raw $\Delta 0$ false preference cross-sensitivity. Although Eq. 2 averages over canonical pairs, the inner average makes it a two-call rate.

Stable cross-sensitivity is the canonical-pair rate of content-stable non-tie choices under order reversal:

$$\text{SCS}(J) = \mathbb{E}_{(u,v) \in \mathcal{D}_0} [\mathbf{1}\{W_J(u, v) = W_J(v, u) \in \{u, v\}\}]. \quad (3)$$

A positional flip occurs when the judge chooses the same slot in both presentation orders, which reverses canonical content identity. Positional false preference is

$$\text{PFP}(J) = \mathbb{E}_{(u,v) \in \mathcal{D}_0} [\mathbf{1}\{J(u, v) = J(v, u) \in \{1, 2\}\}]. \quad (4)$$

This is not a content-stable choice; it indicates presentation-slot driven preference.

The remaining named component is one-sided commit, where exactly one of the two presentation orders yields a non-tie:

$$\text{OSC}(J) = \mathbb{E}_{(u,v) \in \mathcal{D}_0} [\mathbf{1}\{\mathbf{1}\{W_J(u, v) \neq \text{tie}\} + \mathbf{1}\{W_J(v, u) \neq \text{tie}\} = 1\}]. \quad (5)$$

We define the residual other-conflict contribution by subtracting the named components from the pair-level non-tie contribution:

$$\text{Other}(J) = \text{RFP}_0(J) - \text{SCS}(J) - \text{PFP}(J) - \text{OSC}(J)/2. \quad (6)$$

Therefore, under the mutually exclusive canonical-pair classification used for Fig. 3,

$$\text{RFP}_0(J) = \text{SCS}(J) + \text{PFP}(J) + \text{OSC}(J)/2 + \text{Other}(J). \quad (7)$$

The one-half coefficient is fixed by the fact that one-sided commit contributes one non-tie decision across two presentation-order calls. No-preference contributes zero to Eq. 7. For clean outputs restricted to $\{u, v, \text{tie}\}$, stable, positional, one-sided commit, and no-preference exhaust the two-order cases, so Other is zero by construction. We retain Other as a guard category for schema-invalid calls, valid abstentions not mapped to tie, or future protocols with additional non-tie states. In the current clean runs, Other is zero by construction.

For nonzero ladder pairs \mathcal{D}_δ , let $y^*(u, v)$ be the higher-quality content under the prefix-chain construct. The main tables report the all-call target sensitivity, with ties counted as not correct:

$$P_{\text{correct}}^{\text{all}}(\delta; J) = \mathbb{E}_{(u,v,o) \in \mathcal{D}_\delta} [\mathbf{1}\{W_J(o) = y^*(u, v)\}]. \quad (8)$$

When needed, conditional non-tie accuracy is reported separately as

$$P_{\text{correct}}^{\text{non-tie}}(\delta; J) = \Pr [W_J(o) = y^*(u, v) \mid W_J(o) \neq \text{tie}]. \quad (9)$$

Using an isotonic fit $\widehat{P}_{\text{correct}}(\delta)$, the 75 percent detection threshold is

$$\Delta_{75}^*(J) = \inf \left\{ \delta \geq 0 : \widehat{P}_{\text{correct}}(\delta) \geq 0.75 \right\}. \quad (10)$$

If the threshold is reached at the smallest measured nonzero step $\delta = 1$, we report $\Delta_{75}^* \leq 1$ and mark it as left-censored.

We define criterion operationally as the tie operating point induced by prompt p on condition \mathcal{D} :

$$C_J(p; \mathcal{D}) = \Pr [W_J(o; p) = \text{tie} \mid o \in \mathcal{D}], \quad \Delta C = C_J(p_{\text{strict}}; \mathcal{D}) - C_J(p_{\text{base}}; \mathcal{D}). \quad (11)$$

We use criterion operationally as the prompt-induced tie/preference operating point. This is analogous to shifting criterion in signal detection theory, but we do not fit a full parametric SDT model.

Miss-by-tie is the rate at which a target signal exists but the judge returns tie:

$$\text{MBT}(\delta; J) = \Pr [W_J(o) = \text{tie}, y^*(u, v) \text{ exists} \mid (u, v, o) \in \mathcal{D}_\delta]. \quad (12)$$

Algorithm 1: Judge Datasheet Measurement Protocol.

Input: judge J , task set \mathcal{T} , ladder depth L , prompt set $\mathcal{P} = \{p_{\text{base}}, \text{optional } p_{\text{strict}}\}$.

Output: datasheet $d = (\text{DC}, \text{RFP}_0, \text{SCS}, \text{PFP}, \text{OSC}, \text{Other}, P_{\text{correct}}, \Delta_{75}^*, \text{criterion metrics})$.

1. Build the true-vacuum set \mathcal{V} .
2. Measure dark current on \mathcal{V} under the tie-allowed protocol.
3. For each task $t \in \mathcal{T}$, draw a prefix-chain requirement order and construct Q_0, \dots, Q_L with nested requirement sets.
4. Build nonzero ladder pairs \mathcal{D}_δ for $\delta = 1, \dots, L$.
5. Build $\Delta 0$ same-subset and $\Delta 0$ different-subset controls.
6. For each pair, evaluate both presentation orders and map slot outputs back to canonical content identity.
7. Compute raw $\Delta 0$ false preference.
8. Decompose $\Delta 0$ responses into stable cross-sensitivity, positional false preference, one-sided commit, conflict, and no-preference.
9. Compute $P_{\text{correct}}(\delta)$ and Δ_{75}^* .
10. If a strict criterion arm is run, re-evaluate selected pairs under the strict prompt and compute operating-point shift and miss-by-tie.
11. Return the datasheet.

The algorithm is schematic. Exact prompts and JSON schemas are in the appendix and artifacts. This is a measurement protocol, not a model-training algorithm.

A0 true vacuum. The A0 arm measures response in the absence of an evaluative signal according to Eq. 1. A calibrated judge should not manufacture a preference on these inputs. The reported dark current is the false-preference rate under the tie-allowed protocol after schema and semantic validity checks.

A1 controlled quality ladder. The **A1** arm uses a constructively controlled checklist ladder. Each task has a set of required elements. Responses are generated as a prefix chain so that higher levels include a superset of required elements. This yields Pareto-dominant nonzero ΔQ pairs for target-sensitivity measurement. The ladder is intentionally simple: it is not a claim about natural answer quality, but a controlled psychophysical stimulus for the judge.

In the common **A1a** setting, each judge is evaluated on 10 tasks with 60 canonical $\Delta 0$ same-subset pairs and the full prefix-chain nonzero ladder: 50 canonical $\Delta 1$, 40 $\Delta 2$, 30 $\Delta 3$, 20 $\Delta 4$, and 10 $\Delta 5$ pairs, each evaluated in both presentation orders. Publication-facing confidence intervals for call-level proportions use Wilson binomial intervals from the observed numerator and denominator. Task-cluster bootstrap intervals remain in the source artifacts for exploratory diagnostics, but zero-width bootstrap intervals at boundary estimates are not used as publication intervals.

Primary ladder candidates are length-matched within task to avoid conflating checklist cardinality with verbosity. Filler-control pairs separately measure whether a judge rewards or penalizes non-informative filler, and filler variants are not pooled into the primary ΔQ curve. Filler diagnostics are retained as datasheet fields in the source artifacts; no publication-safe common three-judge filler rate is reported in the main table.

$\Delta 0$ controls. The protocol separates $\Delta 0$ same-subset and $\Delta 0$ different-subset pairs. Same-subset pairs hold the target checklist fixed and vary surface form or presentation. Different-subset pairs keep the same cardinality but exchange checklist elements. Raw false preference on $\Delta 0$ pairs follows Eq. 2 and is not automatically cross-sensitivity. For each canonical unordered pair, we collect both presentation orders and map non-tie winners back to canonical candidate identity. A pair is classified as no-preference, stable direction, positional flip, one-sided commit, or other conflict.

Direction-stability decomposition. Stable cross-sensitivity is the stable-direction rate on $\Delta 0$ same-subset pairs in Eq. 3. Positional false preference is the positional-flip rate in Eq. 4: the judge chooses the candidate shown in the same slot under both presentation orders, causing canonical direction to reverse. This distinction is central. A judge can have raw false preference near one while having almost no stable cross-sensitivity if the apparent preference is driven by presentation order.

Target sensitivity and SDT. For nonzero ΔQ pairs, the protocol reports all-call target sensitivity in Eq. 8, tie rate, optional conditional non-tie accuracy in Eq. 9, and the detection threshold in Eq. 10. When the threshold is reached at the smallest measured nonzero step, it is reported as ≤ 1 , not exactly one. The current five-requirement ladder is too coarse to resolve sub-unit thresholds.

Criterion-shift probe. The **A1c-2** probe tightens the tie criterion for Qwen32B according to Eq. 11. This intervention tests whether false preference can be reduced by changing the operating point and whether doing so preserves sensitivity to target differences. Prompting moves the criterion, not the resolution.

4 Results: Three Judges

The main datasheet separates three quantities that are easily conflated. Raw $\Delta 0$ false preference is simply the rate at which a judge refuses to tie on same-quality pairs. Stable cross-sensitivity is

Table 3: Compact Judge Datasheet summary for the three common **A1a** judge runs. Compact values are shown; full confidence intervals and denominators appear in Appendix Table 6. Raw $\Delta 0$ false preference is not cross-sensitivity. Stable cross-sensitivity and positional false preference are canonical-pair decomposition rates after both presentation orders are mapped back to content identity. SCS and PFP are mechanism components, not aliases for raw $\Delta 0$ false preference; the weighted relation including one-sided commit and other conflict is given in Eq. 7. Profile sketches are descriptive summaries for this controlled stimulus family. $\Delta_{75}^* \leq 1$ is left-censored at the smallest measured nonzero ladder step.

Judge	DC	Raw $\Delta 0$ FP	Stable CS	Positional FP	$\Delta 1$	$\Delta 5$	Δ_{75}^*	Profile sketch
Llama8B	0.667	1.000	0.033	0.967	0.610	1.000	4.0	Class B / Presentation-conflicted
Qwen14B	0.000	0.992	0.450	0.533	1.000	1.000	≤ 1	Class A-delta0 / Mixed stable-positional
Qwen32B	0.000	0.258	0.000	0.083	0.940	1.000	≤ 1	Clean Class A

the subset of those decisions that remain content-consistent after presentation order is reversed. Positional false preference is the opposite failure mode: the judge chooses the same slot under both orders, so the canonical content direction flips. Thus raw $\Delta 0$ false preference is a mixture, not a mechanism. Profile sketches are descriptive summaries, not universal taxonomic classes; they summarize the observed profile in this controlled stimulus family.

Table 3 summarizes the main datasheet, with full intervals and denominators in Appendix Table 6. Llama8B has dark current 0.6667 by Eq. 1 and raw $\Delta 0$ false preference 1.0000 by Eq. 2. However, its stable cross-sensitivity is only 0.0333, while positional false preference is 0.9667. This is a Class B / Presentation-conflicted profile: the judge is useful for pipeline debugging, but the $\Delta 0$ response is not stable evidence about surface-form sensitivity.

Qwen14B eliminates true-vacuum dark current and is target-sensitive at both $\Delta 1$ and $\Delta 5$. Its raw $\Delta 0$ false preference is 0.9917, but direction-stability decomposition revises the interpretation. Stable cross-sensitivity by Eq. 3 is 0.4500 and positional false preference by Eq. 4 is 0.5333. Thus, we assign it the descriptive label “**Class A-delta0 / Mixed stable-positional**”. This highlights that high raw false preference should not be conflated with stable cross-sensitivity.

Qwen32B is vacuum-clean, target-sensitive, and has lower $\Delta 0$ artifacts. Its raw $\Delta 0$ false preference is 0.2583, stable cross-sensitivity is 0.0000, positional false preference is 0.0833, and no-preference is 0.5667. In this controlled datasheet it has the cleanest observed profile among the three open-weight judges. This is a descriptive result within this stimulus family, not a universal reliability claim.

The three profiles demonstrate why a scalar win-rate or agreement score is not enough. A high raw same-quality false preference can mean stable sensitivity to nuisance variation, positional false preference, one-sided commit, other conflict, or residual no-preference structure. Raw $\Delta 0$ false preference follows the weighted relation in Eq. 7: stable and positional two-order commitments contribute fully, one-sided commit contributes half, and no-preference contributes zero. These components have different downstream interpretations and require different decisions; Appendix Fig. 5 shows the same decomposition as a positional-vs-stable scatter.

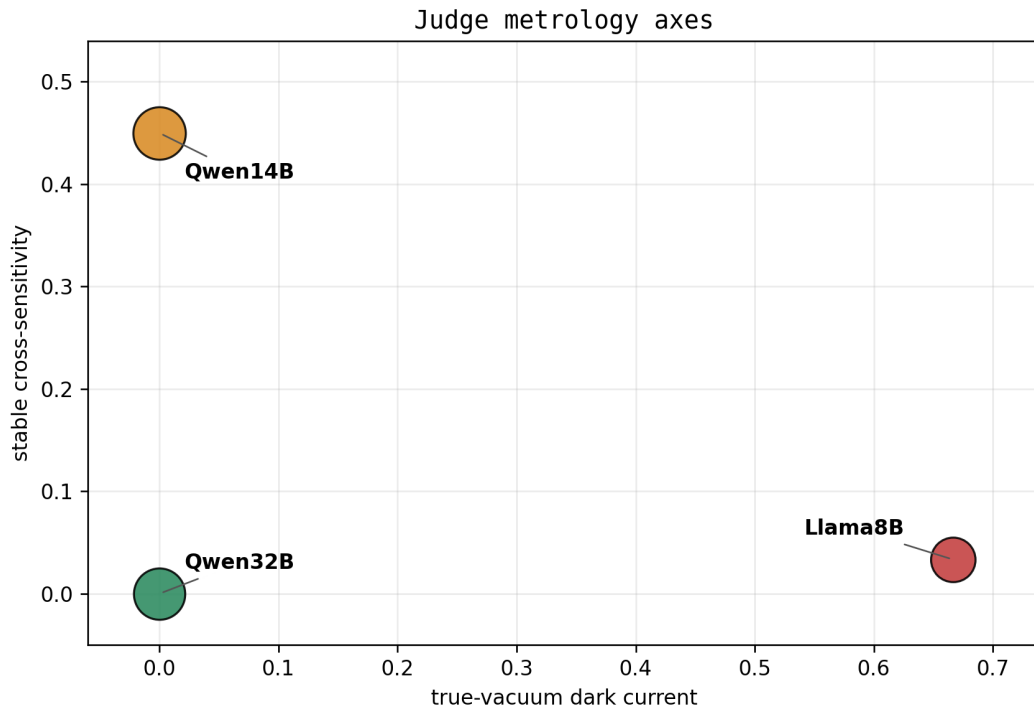


Figure 1: Metrology axes map for the common **A1a** runs. The x-axis is true-vacuum dark current from Eq. 1; the y-axis is stable cross-sensitivity from Eq. 3. Marker size reflects all-call target sensitivity at $\Delta 1$. The strict-criterion arm is excluded because its A0 dark-current arm was not remeasured and is shown only in the operating-point tradeoff in Fig. 4.

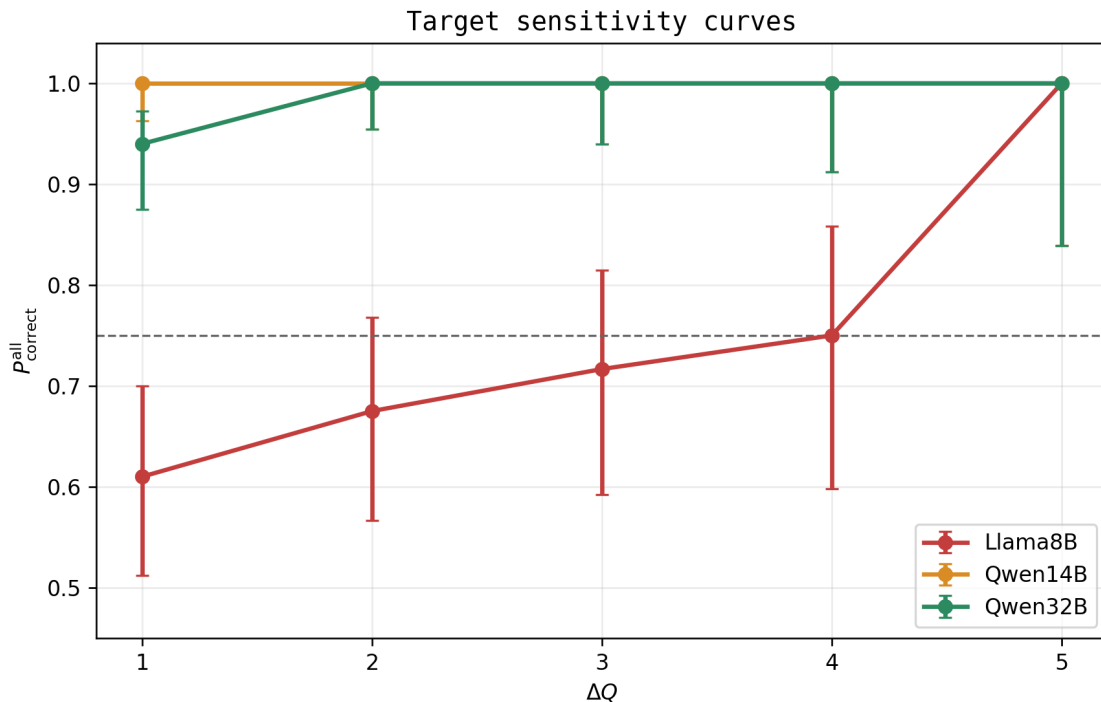


Figure 2: Psychometric target sensitivity curves $P_{\text{correct}}^{\text{all}}(\delta; J)$ from Eq. 8 for the common **A1a** ladder. Error bars use Wilson call-binomial 95 percent intervals computed from observed correct counts and denominators. Qwen14B and Qwen32B reach the 75 percent threshold at the smallest measured nonzero step, so Δ_{75}^* from Eq. 10 is reported as ≤ 1 . Llama8B requires a larger step, with $\Delta_{75}^* = 4.0$ in this run.

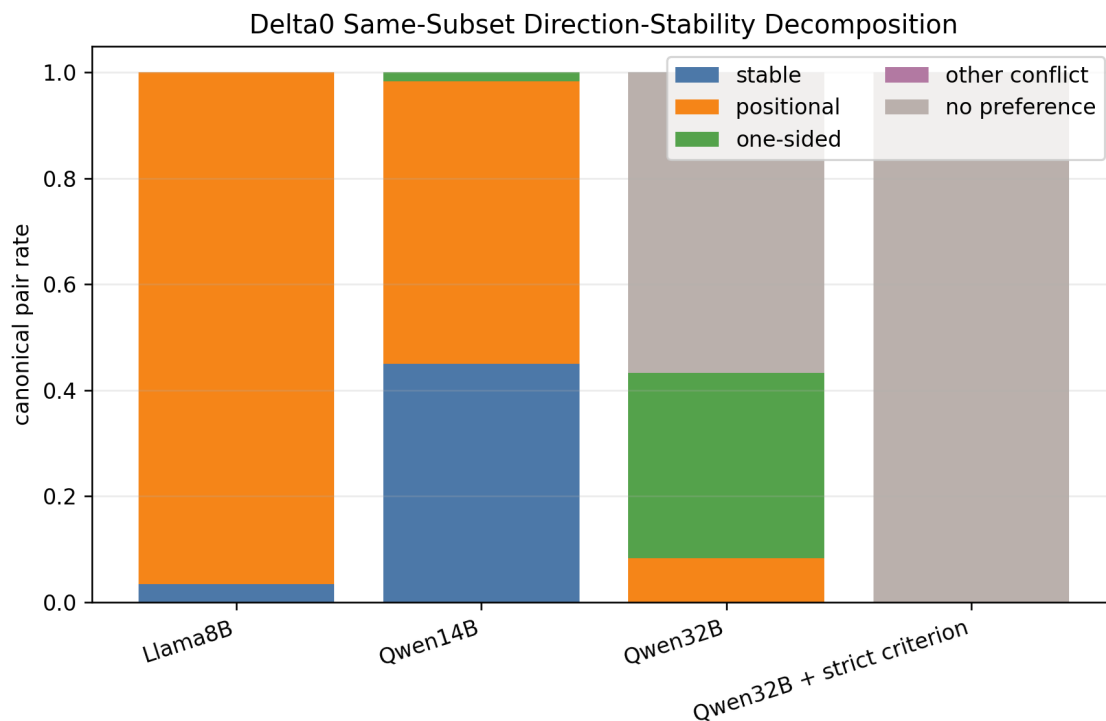


Figure 3: Δ_0 same-subset direction-stability decomposition. Raw false preference from Eq. 2 is not cross-sensitivity; under Eq. 7 it decomposes into stable cross-sensitivity from Eq. 3, positional false preference from Eq. 4, one-sided commit from Eq. 5, other conflict from Eq. 6, and no-preference. The stacked components are canonical-pair components, while raw RFP_0 is a two-call average; one-sided commit enters RFP_0 with a one-half coefficient. Llama8B’s raw false preference is mostly presentation-driven, Qwen14B is mixed, and Qwen32B is low on both stable and positional components. The strict-criterion bar is included only for the Δ_0 same-subset decomposition; A0 dark current was not remeasured under that prompt. Confidence intervals for the decomposed canonical-pair cells are not included in the frozen artifact package and are therefore not inferred here.

5 Criterion Shift

Table 4: Criterion intervention on Qwen32B. The strict prompt eliminates raw $\Delta 0$ false preference, but the lost $\Delta Q = 1$ sensitivity is miss-by-tie rather than wrong-choice error. The $\Delta 0$ no-preference row is a canonical-pair-level decomposition quantity; tie-rate rows are call-level quantities. The strict arm did not run the full threshold protocol, so Δ_{75}^* is not estimated.

Metric	Qwen32B baseline	Qwen32B strict criterion
$\Delta 0$ raw false preference	0.2583 [0.1884, 0.3433]	0.0000 [0.0000, 0.0310]
pair-level $\Delta 0$ no-preference	0.5667	1.0000
$\Delta Q = 1$ target sensitivity	0.9400 [0.8752, 0.9722]	0.5000 [0.4038, 0.5962]
$\Delta Q = 1$ tie rate	0.0600 [0.0278, 0.1248]	0.5000 [0.4038, 0.5962]
$\Delta Q = 1$ wrong-choice rate	0.0000	0.0000
$\Delta Q = 1$ accuracy among non-ties	1.0000	1.0000
$\Delta Q = 5$ target sensitivity	1.0000 [0.8389, 1.0000]	1.0000 [0.8389, 1.0000]
Δ_{75}^*	≤ 1 [left-censored]	N/A

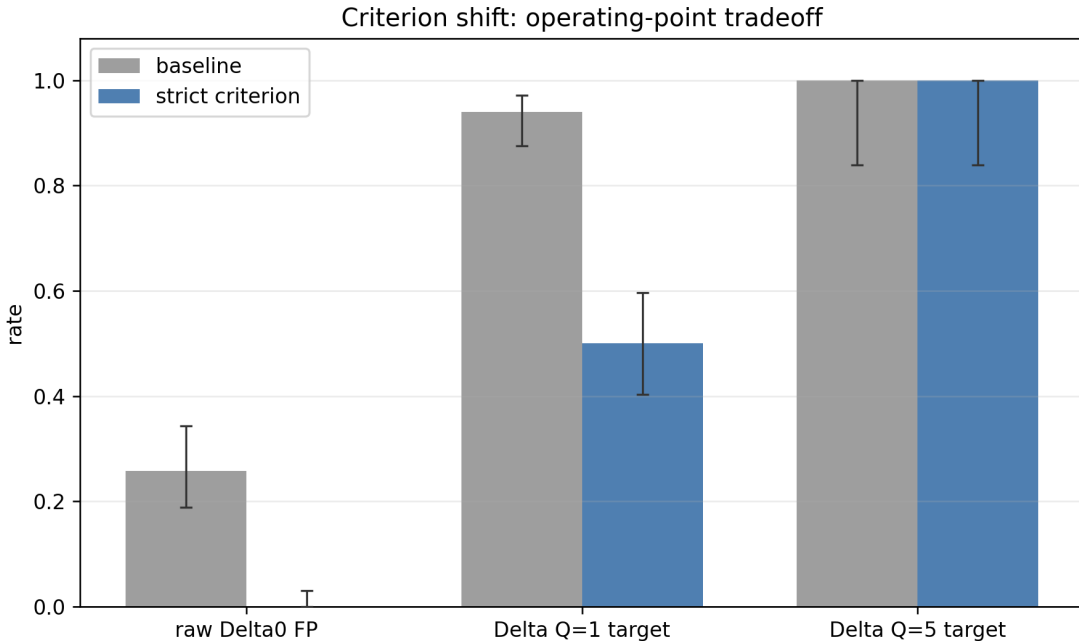


Figure 4: Operating-point tradeoff for Qwen32B under the two-prompt criterion intervention in Eq. 11. This is a two-operating-point segment, not an estimated ROC curve. The strict criterion eliminates raw $\Delta 0$ false preference but absorbs $\Delta Q = 1$ into tie. The $\Delta Q = 1$ errors are miss-by-tie as defined in Eq. 12, not wrong choices: tie rate is 0.5000, wrong-choice rate is 0.0000, and conditional accuracy among non-ties is 1.0000. $\Delta Q = 5$ sensitivity is preserved. Error bars use Wilson call-binomial 95 percent intervals.

The strict tie prompt changes the operating point defined in Eq. 11. Under the baseline protocol, Qwen32B has a call-level $\Delta 0$ same-subset tie rate of 0.7417, corresponding to the pair-level no-preference rate of 0.5667 in Table 4 and Fig. 3; its call-level $\Delta Q = 1$ tie rate is 0.0600, and its

call-level $\Delta Q = 5$ tie rate is 0.0000. Under the strict criterion, raw $\Delta 0$ false preference becomes 0.0000 and pair-level no-preference becomes 1.0000. This is desirable if the goal is to suppress same-quality surface-form over-discrimination.

The $\Delta 0$ tie rate and Fig. 3 no-preference are related but not identical quantities. The tie rate is call-level; no-preference in the decomposition is canonical-pair-level after both orders are collapsed. In the two-order design, one-sided commits contribute one tie and one non-tie call. Thus Qwen32B baseline call-level $\Delta 0$ tie rate 0.7417 is consistent with canonical no-preference 0.5667 plus one half of the one-sided-commit mass.

The cost appears at the margin. $\Delta Q = 1$ target sensitivity falls from 0.9400 to 0.5000. The loss is not a wrong-choice problem: at $\Delta Q = 1$, the wrong-choice rate is 0.0000 and conditional accuracy among non-ties is 1.0000. The low-strength signal is absorbed into tie. At $\Delta Q = 5$, sensitivity remains 1.0000. This pattern supports the criterion interpretation: prompting can move the tie/preference threshold, but it does not create new resolution at low ΔQ .

6 Discussion

Judge datasheets should be run before downstream evaluation claims. A downstream evaluation can be syntactically valid while the judge has high dark current, position-driven false preference, or insufficient target sensitivity. The present case study shows all three possibilities. Llama8B is a strong pipeline-debug judge but a poor calibrated judge for same-quality comparisons. Qwen14B is more sensitive and vacuum-clean, but the direction-stability decomposition shows that raw $\Delta 0$ false preference mixes stable, positional, one-sided, conflict, and no-preference components. Qwen32B has the cleanest profile in this family, but it remains a controlled case-study result rather than a universal guarantee.

The result also clarifies the relationship to the motivating downstream orientation study. If orientation capacity is later modeled as geometry times judge resolvability, the judge-resolvability term cannot be assumed. It must be measured. The current paper supplies that measurement layer. It does not validate the downstream mechanism.

Criterion control is useful but limited. A stricter tie prompt can suppress false positives, but it may also convert weak true positives into no-preference. This resembles changing a detector threshold. The right operating point depends on the downstream use: exploratory ranking may tolerate a lower threshold, while claim-level adjudication requires low dark current and explicit uncertainty about low-strength signals.

A future phase should use a stronger external comparator or reference judge as a ceiling estimate, not as ground truth. It should also refine the ladder below one requirement, because $\Delta_{75}^* \leq 1$ is left-censored in the present design. Finally, the protocol should be extended across model families and naturalistic answer domains before any generality claim is made.

7 Limitations

The stimulus ladder is synthetic. Its strength is constructive control, not ecological completeness. Same-quality surface differences may be genuinely visible to humans, and cross-sensitivity is not always bad. In some applications, style, specificity, or clarity are part of the target construct. The present protocol treats them as nuisance axes only because the controlled task defines the checklist as the target.

There is no human ground truth or reference/API judge in the reported runs. Future reference-judge work should be treated as a ceiling or external comparator, not as ground truth. Qwen32B

Table 5: Explicit non-claims maintained in the draft.

Non-claim	Reason
The downstream mechanism hypothesis is not confirmed.	Those downstream experiments were not executed in this phase.
The original orientation mechanism is not validated.	This paper measures judges, not the downstream mechanism.
Qwen32B is not established as a general-purpose evaluator.	It is a strong comparator in this controlled datasheet only.
No broad size-family trend is claimed.	Three open-weight judges are a case study, not a trend sample.
Reference/API judges are not ground truth.	Future reference runs are ceilings or external comparators.

is not claim-level evidence for the downstream mechanism hypothesis. It is a cleaner measurement instrument in this controlled datasheet.

The Δ_{75}^* values for Qwen14B and Qwen32B are left-censored. The current ladder measures integer requirement differences. If a judge reaches 75 percent at the smallest nonzero step, the threshold is ≤ 1 , not exactly one. Finer perturbations are required to compare sub-unit sensitivity.

The case study uses three open-weight judges. This is insufficient for broad family-level claims. The results should be read as a demonstration of metrological profiling and as evidence that scalar judge scores can hide distinct failure modes.

This paper establishes the metrology base for LLM evaluation under highly controlled conditions. Future work will extend this Judge Datasheet protocol to large-scale, naturalistic NLP benchmarks, such as RewardBench [12], to evaluate its ecological validity and operational cost-performance in production environments.

8 Conclusion

LLM judges are measurement instruments. They can have dark current, positional false preference, stable cross-sensitivity, target sensitivity, and criterion shifts. Reporting only accuracy, win-rate, or agreement hides these axes. We introduced a Judge Datasheet protocol that measures true-vacuum response, controlled target sensitivity, direction-stability under $\Delta 0$ same-quality pairs, and criterion tradeoffs. In a three-judge case study, Llama8B, Qwen14B, and Qwen32B occupy different profiles that would be collapsed by scalar reporting. Before a judge is used to support downstream scientific claims, the measuring device itself should be measured.

Artifact Statement

This arXiv version does not include a separate public artifact release. The submission source package contains only the files required to build the manuscript. The reported experiments use controlled synthetic stimuli and aggregate outputs; raw call/response logs, service endpoints, local absolute paths, and environment-specific operational traces are not distributed.

The prompt structure, output schema, stimulus design, denominators, confidence intervals, and numerical audit information needed to assess the reported claims are described in the manuscript and appendix. Additional reproducibility materials may be provided under the policy of a future peer-review venue.

AI Usage Statement

The authors used AI-assisted tools in a controlled research workflow for brainstorming, implementation support, code refactoring, draft organization, language polishing, and internal critique. The reported experimental calls were executed through logged scripts on controlled local or self-hosted infrastructure unless explicitly stated otherwise. All experimental designs, model outputs, numerical results, claims, citations, and final text were inspected and verified by the human authors. AI systems were not authors and are not responsible for the content. The human authors take full responsibility for the accuracy, integrity, and originality of the manuscript.

Acknowledgments

This work was conducted in part within a collaborative research context between Chubu University and Mitsubishi Heavy Industries, Ltd., Research & Innovation Center. We thank members of the Research & Innovation Center for discussions on AI-cluster operation, hardware-configuration constraints, and deployment-oriented evaluation settings. These discussions helped motivate the need to treat LLM judges as measurement instruments rather than scalar scorers. The judge-metrology protocol, stimulus construction, model-call execution, analysis scripts, numerical audits, and manuscript claims reported in this paper were developed and verified by the authors. The reported experiments use controlled synthetic stimuli and logged local or self-hosted inference infrastructure; they do not rely on proprietary deployment data, confidential site logs, or non-public hardware-integration details.

A Appendix

A.1 Protocol details

The A0 protocol uses true-vacuum pairs: empty strings, whitespace-only candidates, and identical non-empty candidates. The A1 protocol uses a prefix-chain checklist ladder. Each task has required elements; quality level is the number of included elements under a fixed ordering. Primary nonzero pairs compare levels separated by ΔQ . $\Delta 0$ same-subset pairs compare surface variants of the same included set. $\Delta 0$ different-subset pairs compare equal-cardinality but different included sets.

A.2 Glossary

Judge Datasheet. A structured report of evaluator behavior across dark current, raw $\Delta 0$ false preference, stable cross-sensitivity, positional false preference, target sensitivity, threshold, and criterion; interpretive summary built from measured quantities.

True vacuum. Inputs with no evaluative signal, including empty, whitespace, and identical non-empty candidate pairs; constructed stimulus condition.

Valid abstention. A parser- and schema-valid no-decision output when the protocol permits abstention; measured output category.

No-preference. Tie or valid abstention depending on the protocol and table level; measured output category.

$\Delta 0$ same-subset. Same-quality pairs with the same checklist subset and surface-form variation; constructed control condition.

$\Delta 0$ different-subset. Same-cardinality pairs with different checklist elements; constructed control condition.

Prefix-chain ladder. A nested response family in which higher levels include a superset of required elements; constructed stimulus ladder.

Pareto dominance, construct-relative. The relation that higher ladder levels contain all lower-level checklist elements plus more under the defined construct; constructed relation, not a universal quality claim.

Raw $\Delta 0$ false preference. The call-level non-tie rate on same-quality pairs; measured quantity and not a mechanism by itself.

Stable cross-sensitivity. A canonical-pair-level content-stable direction under order reversal; measured decomposition quantity interpreted as nuisance in this checklist construct.

Positional false preference. A canonical-pair-level same-slot choice under order reversal; measured decomposition quantity indicating slot-driven preference.

One-sided commit. A canonical-pair-level component where exactly one presentation order yields a non-tie decision; measured decomposition quantity contributing one half to raw $\Delta 0$ false preference.

Other conflict. The residual other-conflict contribution after stable cross-sensitivity, positional false preference, and one-sided commit are accounted for; measured decomposition quantity under the frozen classification.

Target sensitivity. Correct selection of the Pareto-dominant candidate on nonzero ladder pairs; measured call-level quantity.

Δ_{75}^* . The smallest ladder difference at which isotonic target sensitivity reaches 0.75; fitted ladder-level quantity.

Left-censoring. A threshold reported as ≤ 1 because the first measured nonzero ladder step already reaches the threshold; interpretive flag from the ladder design.

Criterion / operating point. The prompt-induced tie/preference boundary, operationalized as tie rate by condition; measured condition-level quantity.

Miss-by-tie. A target signal not selected because the judge returns tie; measured call-level error mode.

Presentation-conflicted. A profile sketch where raw $\Delta 0$ false preference is dominated by presentation-order conflict or slot effects; interpretive label for this stimulus family.

External comparator / ceiling estimate. A stronger or reference judge used for comparison, not as ground truth; interpretive role for future work.

Downstream mechanism hypothesis. The motivating orientation hypothesis outside the present judge-metrology paper; interpretive context, not tested here.

A.3 Length and filler controls

Primary ladder candidates are length-matched within task. Filler variants are diagnostic controls for verbosity or filler preference and are not pooled into the primary ΔQ curve. The frozen working-snapshot artifact package (frozen WS package) does not expose a common three-judge filler-clean preference value suitable for the main datasheet table.

A.4 Prompt templates

The baseline pair-tie-allowed prompt instructs the judge that the two candidates may be equally good and allows a tie. The strict criterion prompt strengthens the instruction to choose tie whenever differences are only wording, style, fluency, verbosity, or surface form. The artifact package contains prompt templates, output JSON schemas, prompt-rendering code, stimulus manifests, and redacted rendered-prompt records sufficient to reconstruct the prompts used in the reported runs. Full unredacted service logs are retained only in the internal frozen package for audit and are not part of the public release. The prompt construction does not expose expected winners, ΔQ labels, quality levels, or canonical-pair metadata to the judge prompt.

A.5 Prefix-chain dominance

For primary ladder pairs, higher levels include a superset of checklist elements. Under the task construct, this yields a constructive Pareto dominance relation. This proof is construct-relative: it does not imply that natural answer quality is fully captured by checklist cardinality.

A.6 Metric definitions

Main metric definitions are given in Eqs. 1–11 and Eq. 12. The important implementation detail is that slot outputs are mapped back to canonical content identity before direction-stability quantities are computed. Raw $\Delta 0$ false preference is a call-level non-tie rate and is not treated as stable cross-sensitivity.

A.7 Confidence intervals

Publication-facing call-level proportions use Wilson binomial 95 percent intervals computed from the observed numerator and denominator. This applies to dark current, raw $\Delta 0$ false preference, tie rates, and nonzero target-sensitivity proportions, including boundary estimates. Task-cluster bootstrap intervals are retained in the source artifacts for diagnostics, but zero-width bootstrap intervals at observed 0 or 1 are not printed as publication intervals. Cells without a valid design denominator are reported as N/A with a reason. No confidence intervals are invented in this draft. Stable cross-sensitivity and positional false preference CIs are N/A because the frozen package includes canonical-pair decomposition counts but not decomposition-level bootstrap intervals.

Table 6: Full confidence-interval and denominator table for the reported datasheet metrics. Values marked N/A were not measured or not estimable in the frozen artifact. Raw delta0 false preference rows are call-level non-tie rates and should not be read as stable cross-sensitivity. Stable cross-sensitivity and positional false preference rows are canonical-pair decomposition rates; decomposition-level bootstrap intervals were not included in the frozen package and are not invented here. For Qwen14B and Qwen32B, Δ_{75}^* is displayed as ≤ 1 [left-censored]; the underlying numeric plotting value in the frozen artifact is 1.0000.

Judge	Metric	Estimate	95% CI	n	Method or reason
Llama8B	dark current false preference	0.6667	[0.5783, 0.7447]	120	Wilson binomial
Llama8B	raw delta0 false preference	1.0000	[0.9690, 1.0000]	120	Wilson binomial
Llama8B	$\Delta 0$ tie rate	0.0000	[0.0000, 0.0310]	120	Wilson binomial
Llama8B	target sensitivity $\Delta 1$	0.6100	[0.5120, 0.6998]	100	Wilson binomial
Llama8B	$\Delta 1$ tie rate	0.0000	[0.0000, 0.0370]	100	Wilson binomial
Llama8B	target sensitivity $\Delta 5$	1.0000	[0.8389, 1.0000]	20	Wilson binomial
Llama8B	$\Delta 5$ tie rate	0.0000	[0.0000, 0.1611]	20	Wilson binomial
Llama8B	Δ_{75}^*	4.0000	[2.7143, 4.0000]	300	source bootstrap; censor flag
Llama8B	d' at $\Delta 5$	3.3812	N/A	20	ceiling d-prime; CI N/A
Qwen14B	dark current false preference	0.0000	[0.0000, 0.0310]	120	Wilson binomial
Qwen14B	raw delta0 false preference	0.9917	[0.9543, 0.9985]	120	Wilson binomial
Qwen14B	$\Delta 0$ tie rate	0.0083	[0.0015, 0.0457]	120	Wilson binomial
Qwen14B	target sensitivity $\Delta 1$	1.0000	[0.9630, 1.0000]	100	Wilson binomial
Qwen14B	$\Delta 1$ tie rate	0.0000	[0.0000, 0.0370]	100	Wilson binomial
Qwen14B	target sensitivity $\Delta 5$	1.0000	[0.8389, 1.0000]	20	Wilson binomial
Qwen14B	$\Delta 5$ tie rate	0.0000	[0.0000, 0.1611]	20	Wilson binomial
Qwen14B	Δ_{75}^*	≤ 1 [left-censored]	N/A	300	source bootstrap; censor flag

Continued on next page.

Table 6: Full confidence-interval and denominator table, continued.

Judge	Metric	Estimate	95% CI	n	Method or reason
Qwen14B	d' at $\Delta 5$	3.3812	N/A	20	ceiling d-prime; CI N/A
Qwen32B	dark current false preference	0.0000	[0.0000, 0.0310]	120	Wilson binomial
Qwen32B	raw delta0 false preference	0.2583	[0.1884, 0.3433]	120	Wilson binomial
Qwen32B	$\Delta 0$ tie rate	0.7417	[0.6567, 0.8116]	120	Wilson binomial
Qwen32B	target sensitivity $\Delta 1$	0.9400	[0.8752, 0.9722]	100	Wilson binomial
Qwen32B	$\Delta 1$ tie rate	0.0600	[0.0278, 0.1248]	100	Wilson binomial
Qwen32B	target sensitivity $\Delta 5$	1.0000	[0.8389, 1.0000]	20	Wilson binomial
Qwen32B	$\Delta 5$ tie rate	0.0000	[0.0000, 0.1611]	20	Wilson binomial
Qwen32B	Δ_{75}^*	≤ 1 [left-censored]	N/A	300	source bootstrap; censor flag
Qwen32B	d' at $\Delta 5$	3.3812	N/A	20	ceiling d-prime; CI N/A
Qwen32B strict criterion	dark current false preference	N/A	N/A	N/A	not measured in strict criterion probe
Qwen32B strict criterion	raw delta0 false preference	0.0000	[0.0000, 0.0310]	120	Wilson binomial
Qwen32B strict criterion	$\Delta 0$ tie rate	1.0000	[0.9690, 1.0000]	120	Wilson binomial
Qwen32B strict criterion	target sensitivity $\Delta 1$	0.5000	[0.4038, 0.5962]	100	Wilson binomial
Qwen32B strict criterion	$\Delta 1$ tie rate	0.5000	[0.4038, 0.5962]	100	Wilson binomial
Qwen32B strict criterion	target sensitivity $\Delta 5$	1.0000	[0.8389, 1.0000]	20	Wilson binomial
Qwen32B strict criterion	$\Delta 5$ tie rate	0.0000	[0.0000, 0.1611]	20	Wilson binomial
Qwen32B strict criterion	Δ_{75}^*	N/A	N/A	N/A	strict criterion probe has Delta=1 and Delta=5 only
Qwen32B strict criterion	d' at $\Delta 5$	3.3812	N/A	20	ceiling d-prime; CI N/A
Llama8B	stable cross-sensitivity decomposition	0.0333	N/A	60	canonical-pair decomposition; CI N/A
Llama8B	positional false preference decomposition	0.9667	N/A	60	canonical-pair decomposition; CI N/A
Qwen14B	stable cross-sensitivity decomposition	0.4500	N/A	60	canonical-pair decomposition; CI N/A
Qwen14B	positional false preference decomposition	0.5333	N/A	60	canonical-pair decomposition; CI N/A
Qwen32B	stable cross-sensitivity decomposition	0.0000	N/A	60	canonical-pair decomposition; CI N/A
Qwen32B	positional false preference decomposition	0.0833	N/A	60	canonical-pair decomposition; CI N/A
Qwen32B + strict criterion	stable cross-sensitivity decomposition	0.0000	N/A	60	canonical-pair decomposition; CI N/A
Qwen32B + strict criterion	positional false preference decomposition	0.0000	N/A	60	canonical-pair decomposition; CI N/A

Table 7: Full metric-reference table with protocol and denominator. Bad direction is construct-relative; some axes, especially stable cross-sensitivity and criterion, require downstream interpretation rather than a universal good/bad sign.

Term	Symbol	Level	Protocol / denominator	Measures	Bad direction
Dark current	DC	call	tie-allowed true vacuum; true-vacuum calls	false preference with no evaluative signal	higher
Raw $\Delta 0$ false preference	RFP ₀	call	tie-allowed $\Delta 0$ same; both-order calls	any non-tie on same-quality same-subset pairs; raw, not cross-sensitivity	higher
Stable cross-sensitivity	SCS	canonical pair	tie-allowed $\Delta 0$ same, both orders; canonical $\Delta 0$ same pairs	content-stable direction under surface variation	construct-dependent
Positional false preference	PFP	canonical pair	tie-allowed $\Delta 0$ same, both orders; canonical $\Delta 0$ same pairs	same presentation-slot choice under order reversal	higher
No-preference	NP	call or pair	tie-allowed; relevant calls or pairs	tie or valid abstention	construct-dependent
Target sensitivity	P_{corr}	call	pair protocol in caption; nonzero ΔQ calls	correct selection of the Pareto-dominant prefix-chain candidate	lower
Detection threshold	Δ_{75}^*	ladder fit	target-sensitivity curve; ladder curve	smallest ΔQ where isotonic target sensitivity reaches 0.75	higher
Criterion / operating point	C_J / tie rate	condition	baseline vs strict prompt; condition-specific calls	prompt-induced tie/preference boundary	no universal direction
Miss-by-tie	MBT	call	tie-allowed target pairs; target ΔQ calls	target signal not selected because the judge returns tie	higher when signal should be detected

A.8 Supplementary decomposition view

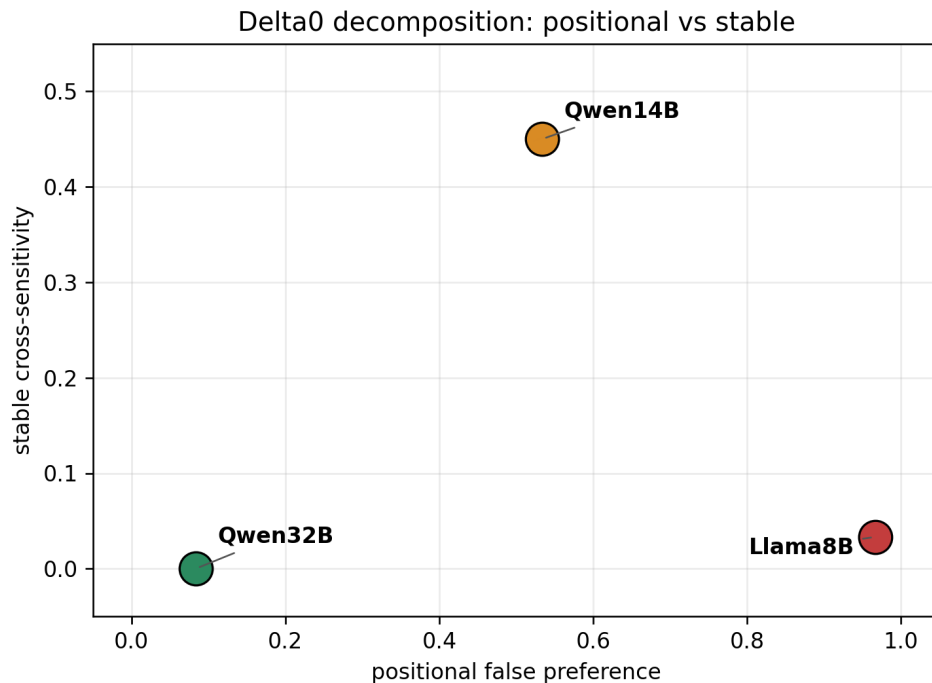


Figure 5: Supplementary positional false preference versus stable cross-sensitivity scatter for $\Delta 0$ same-subset pairs. Raw $\Delta 0$ false preference decomposes into distinct mechanisms: Llama8B is mostly positional, Qwen14B is mixed, and Qwen32B is low on both stable and positional components.

A.9 Prior mini-experiment reclassification

The previous downstream mini-experiment is not treated as evidence for the motivating mechanism hypothesis. It is reclassified as a motivation for measuring the judge before downstream claim testing.

A.10 Future plan

The next phase should introduce an external comparator or reference judge as a ceiling estimate, refine the ladder below one requirement, and maintain the separation between judge metrology and downstream mechanism claims.

References

- [1] Junhyuk Choi, Sohhyung Park, Chanhee Cho, Hyeonchu Park, and Bugeun Kim. Diagnosing the reliability of LLM-as-a-Judge via item response theory. arXiv preprint arXiv:2602.00521, 2026.
- [2] Percy Liang, Rishi Bommasani, Tony Lee, Dimitris Tsipras, Dilara Soylu, Michihiro Yasunaga, Yian Zhang, Deepak Narayanan, Yuhuai Wu, Ananya Kumar, Benjamin Newman, Binhang Yuan, Bobby Yan, Ce Zhang, Christian Cosgrove, Christopher D. Manning, Christopher Ré, Diana Acosta-Navas, Drew A. Hudson, Eric Zelikman, et al. Holistic Evaluation of Language Models. *Transactions on Machine Learning Research*, 2023. HELM.
- [3] Aarohi Srivastava, Abhinav Rastogi, Abhishek Rao, Abu Awal Md Shoeb, Abubakar Abid, Adam Fisch, Adam R. Brown, Adam Santoro, Aditya Gupta, Adrià Garriga-Alonso, et al. Beyond the Imitation Game: Quantifying and Extrapolating the Capabilities of Language Models. *Transactions on Machine Learning Research*, 2023. BIG-Bench.
- [4] Lianmin Zheng, Wei-Lin Chiang, Ying Sheng, Siyuan Zhuang, Zhanghao Wu, Yonghao Zhuang, Zi Lin, Zhuohan Li, Dacheng Li, Eric P. Xing, Hao Zhang, Joseph E. Gonzalez, and Ion Stoica. Judging LLM-as-a-Judge with MT-Bench and Chatbot Arena. In *Advances in Neural Information Processing Systems*, volume 36, pages 46595–46623. Curran Associates, Inc., 2023.
- [5] Yann Dubois, Balázs Galambosi, Percy Liang, and Tatsunori B. Hashimoto. Length-Controlled AlpacaEval: A Simple Way to Debias Automatic Evaluators. In *First Conference on Language Modeling*, 2024. arXiv:2404.04475.
- [6] OpenAI. Evals. <https://github.com/openai/evals>, 2023. Software framework.
- [7] Jon-Paul Cacioli. LLMs as signal detectors: Sensitivity, bias, and the temperature-criterion analogy. arXiv preprint arXiv:2603.14893, 2026.
- [8] Lin Shi, Chiyu Ma, Wenhua Liang, Xingjian Diao, Weicheng Ma, and Soroush Vosoughi. Judging the judges: A systematic study of position bias in LLM-as-a-Judge. arXiv preprint arXiv:2406.07791, 2024.
- [9] Jinming Yang, Zheng Hu, Chuxian Qiu, Zhenyu Deng, Xinshan Jiao, and Tao Zhou. Quantifying and mitigating self-preference bias of LLM judges. arXiv preprint arXiv:2604.22891, 2026.
- [10] Timnit Gebru, Jamie Morgenstern, Briana Vecchione, Jennifer Wortman Vaughan, Hanna Wallach, Hal Daumé III, and Kate Crawford. Datasheets for Datasets. *Communications of the ACM*, 64(12):86–92, 2021.
- [11] Margaret Mitchell, Simone Wu, Andrew Zaldivar, Parker Barnes, Lucy Vasserman, Ben Hutchinson, Elena Spitzer, Inioluwa Deborah Raji, and Timnit Gebru. Model Cards for Model Reporting. In *Proceedings of the Conference on Fairness, Accountability, and Transparency*, pages 220–229. ACM, 2019.
- [12] Nathan Lambert, Valentina Pyatkin, Jacob Morrison, LJ Miranda, Bill Yuchen Lin, Khyathi Chandu, Nouha Dziri, Sachin Kumar, Tom Zick, Yejin Choi, Noah A. Smith, and Hannaneh Hajishirzi. RewardBench: Evaluating Reward Models for Language Modeling. In *Findings of the Association for Computational Linguistics: NAACL 2025*, pages 1755–1797, Albuquerque, New Mexico, 2025. Association for Computational Linguistics.